

Interplay between static cooperative Jahn–Teller distortion and magnetic properties of optimally doped manganites

This article has been downloaded from IOPscience. Please scroll down to see the full text article.

2004 J. Phys.: Condens. Matter 16 9031

(<http://iopscience.iop.org/0953-8984/16/49/018>)

View [the table of contents for this issue](#), or go to the [journal homepage](#) for more

Download details:

IP Address: 129.252.86.83

The article was downloaded on 27/05/2010 at 19:25

Please note that [terms and conditions apply](#).

Interplay between static cooperative Jahn–Teller distortion and magnetic properties of optimally doped manganites

D P Kozlenko^{1,2} and B N Savenko¹

¹ Frank Laboratory of Neutron Physics, JINR, 141980 Dubna Moscow Region, Russia

² ISIS Facility, Rutherford Appleton Laboratory, Chilton, Didcot, Oxon OX11 0QX, UK

Received 7 September 2004, in final form 26 October 2004

Published 26 November 2004

Online at stacks.iop.org/JPhysCM/16/9031

doi:10.1088/0953-8984/16/49/018

Abstract

An effect of the static long range cooperative Jahn–Teller (JT) distortion on the magnetic properties of $A_{0.7}A'_{0.3}\text{MnO}_3$ ($A = \text{La, Pr, Nd}$; $A' = \text{Ca, Sr}$) manganites with the orthorhombic structure of $Pnma$ symmetry is studied on the basis of structural, magnetic and transport properties data. A direct relationship between the static JT distortion parameter and the Curie temperature was found. The relationship between the static long range cooperative JT distortion, strength of electron–phonon coupling effects and magnetic properties of $A_{0.7}A'_{0.3}\text{MnO}_3$ manganites is discussed.

1. Introduction

Manganites of perovskite type $A_{1-x}A'_x\text{MnO}_3$ (A —rare earth, A' —alkali earth elements) exhibit rich magnetic and electronic phase diagrams depending on the A-site elements and their ratio, and they have attracted considerable interest with respect to the recently discovered colossal magnetoresistance (CMR) effect [1]. For the optimum doping range $x \sim 0.3$, manganites generally exhibit a ferromagnetic metallic state below the Curie temperature T_C which is governed by the double-exchange interaction [2–4]. The ferromagnetic arrangement of the localized t_{2g} spins is mediated by the itinerant e_g electrons via the on-site Hund's rule coupling J_H . The magnetic and transport properties of double-exchange ferromagnets are controlled by the one-electron bandwidth W , which is proportional to the Mn–O–Mn electron transfer integral, and $T_C \propto W$ in the strong coupling limit ($J_H \gg W$) [5].

The bandwidth can be effectively tuned by the 'internal' pressure (variation of the average A-site ionic radius $\langle r_A \rangle$) or high external pressure [6–9]. Both the increase of $\langle r_A \rangle$ and the application of high external pressure lead to the increase of T_C . The variation of the bandwidth due to the structural effects can be expressed as

$$W \propto \frac{\cos^2 \theta}{l_{\text{Mn-O}}^{3.5}}, \quad (1)$$

Table 1. JT distortion parameters, Curie temperatures, activation energies, average A-site ionic radii, Mn–O bond lengths and Mn–O–Mn bond angles for $A_{0.7}A'_{0.3}MnO_3$ manganites.

	δ_{JT} (Å)	T_C (K)	E_a (meV)	$\langle r_A \rangle$ (Å)	l_{Mn-O} (Å)	θ (deg)
$La_{0.7}Ca_{0.17}Sr_{0.13}MnO_3$ [12, 16]	0.0003	309	—	1.222	1.959	163.04
$La_{0.7}Ca_{0.3}MnO_3$ [13, 8]	0.0019	270	131.6	1.205	1.962	160.53
$Pr_{0.7}Sr_{0.3}MnO_3$ [14]	0.0023	259	—	1.218	1.962	160.91
$Nd_{0.7}Sr_{0.3}MnO_3$ [15]	0.0053	210	142.8	1.207	1.962	159.5
$La_{0.525}Pr_{0.175}Ca_{0.3}MnO_3$ [12, 6]	0.0066	200	147.2	1.199	1.963	159.18
$Nd_{0.7}Ca_{0.22}Sr_{0.08}MnO_3$ [15]	0.0129	130	165.6	1.179	1.965	156.29

where l_{Mn-O} is the Mn–O bond length and θ is the Mn–O–Mn bond angle [7, 9, 10].

However, recent analysis of $A_{1-x}A'_xMnO_3$ manganites with $x = 1/3$ has shown that consideration of structural effects only does not allow one to explain the observed variation of T_C as a function of $\langle r_A \rangle$, and electron–phonon coupling effects arising from Jahn–Teller (JT) structural distortion were found to be important [7]. The formation of polarons due to the strong electron–phonon coupling effects leads to further reduction of the bare bandwidth

$$W_{\text{eff}} = W \exp(-\gamma E_{JT}/\hbar\omega), \quad (2)$$

where E_{JT} is the Jahn–Teller polaron binding energy, ω is the characteristic phonon frequency and parameter $0 < \gamma < 1$ depends on $E_{JT}/\hbar\omega$. An increase of the $\gamma E_{JT}/\hbar\omega$ value with $\langle r_A \rangle$ decrease was found [7].

The electron–phonon coupling effects are especially pronounced in the optimally doped manganites with the orthorhombic crystal structure with $Pnma$ symmetry and relatively small $\langle r_A \rangle < 1.22$ Å where a static long range cooperative JT distortion is present. Such effects are strongly reduced for compounds with the rhombohedral structure of $R\bar{3}c$ symmetry ($\langle r_A \rangle > 1.22$ Å), as found in the study of compounds $La_{2/3}(Ca_{1-x}Sr_x)MnO_3$ [11]. In the latter case the static long range cooperative JT distortion is forbidden by the symmetry and the relevant electron–phonon coupling effects become negligible.

From the above reasons one would expect close correlation between the parameters characterizing the static long range cooperative JT distortion and electron–phonon coupling effects in the orthorhombic manganites. In this paper, interplay between the static long range cooperative JT distortion and the magnetic properties of optimally doped orthorhombic manganites $A_{0.7}A'_{0.3}MnO_3$ ($A = La, Pr, Nd$; $A' = Ca, Sr$) is studied using available experimental data [6, 12–16].

2. Results and discussion

In the orthorhombic structure of $Pnma$ symmetry there are three nonequivalent pairs of Mn–O bonds (Mn–O₁, Mn–O_{2a} and MnO_{2b}), and the static long range cooperative JT distortion of MnO_6 octahedra is characterized by the parameter [12]

$$\delta_{JT} = \sqrt{\frac{1}{3} \sum_i [(l_{Mn-O})_i - \langle l_{Mn-O} \rangle]^2}, \quad (3)$$

where the summation index $i = 1 \dots 3$ corresponds to particular Mn–O bond lengths l_{Mn-O} .

The δ_{JT} values calculated from the structural data at ambient temperature [12–15] for the $A_{0.7}A'_{0.3}MnO_3$ compounds considered are presented in table 1 along with the corresponding T_C values.

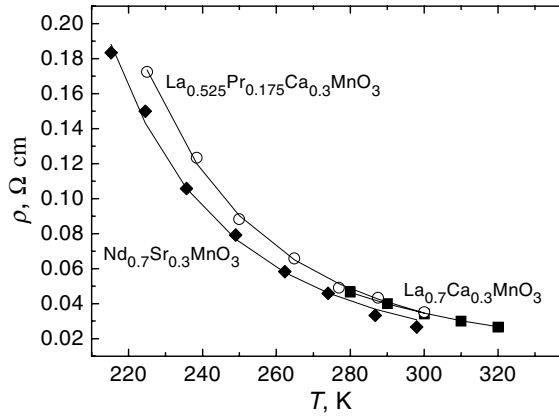


Figure 1. Temperature dependences of resistivity of $\text{La}_{0.7}\text{Ca}_{0.3}\text{MnO}_3$ [6], $\text{La}_{0.525}\text{Pr}_{0.175}\text{Ca}_{0.3}\text{MnO}_3$ [8] and $\text{Nd}_{0.7}\text{Sr}_{0.3}\text{MnO}_3$ [15] in the $T > T_C$ region and their fit by the function (4) (solid curves). The error bars are within the symbol sizes.

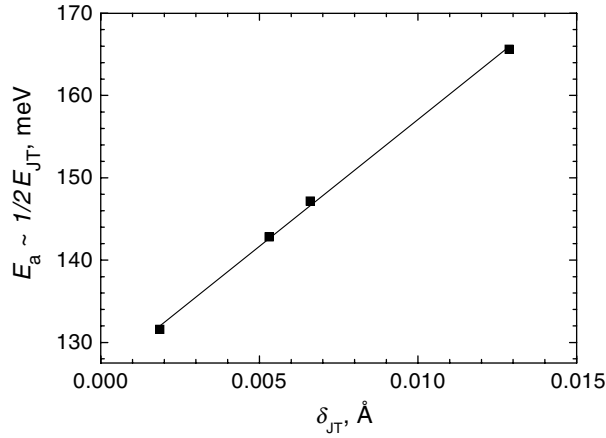


Figure 2. Activation energy $E_a \approx \frac{1}{2}E_{JT}$ as a function of static JT distortion parameter in $\text{A}_{0.7}\text{A}'_{0.3}\text{MnO}_3$ manganites. The solid line represents a linear fit to the experimental data. The error bars are within the symbol sizes.

In the adiabatic polaron hopping limit which is found to be appropriate for manganites [17] the temperature behaviour of resistivity above T_C is defined by

$$\rho \propto (kT/\hbar\omega) \exp(E_a/kT), \quad (4)$$

where the activation energy is $E_a = \frac{1}{2}E_{JT} - \frac{W}{2z}$, the bare bandwidth W is defined by (1), z is the lattice coordination number and k is the Boltzmann constant [18]. The values of E_a obtained for selected $\text{A}_{0.7}\text{A}'_{0.3}\text{MnO}_3$ manganites from the analysis of resistivity data [6, 8, 14, 15] (figure 1) are presented in table 1. The variation of bare bandwidth W for the studied compounds does not exceed 10%, as can be estimated from table 1 using equation (1). Thus, the observed variation of activation energy (table 1) comes mainly from the change of the $\frac{1}{2}E_{JT}$ term, and $E_a \approx \frac{1}{2}E_{JT}$. The E_{JT} value increases linearly with the increase of the static JT distortion parameter δ_{JT} (figure 2). The Curie temperature in $\text{A}_{0.7}\text{A}'_{0.3}\text{MnO}_3$ manganites exhibits a nonlinear decrease with increase of the δ_{JT} parameter (figure 3). Assuming $T_C \propto W_{\text{eff}}$, it

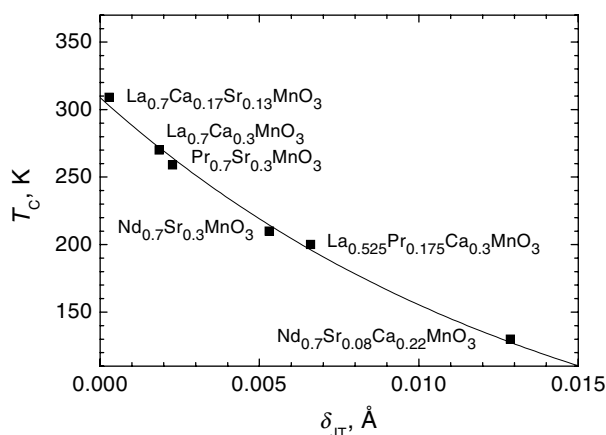


Figure 3. Dependence of the Curie temperature on the static JT distortion parameter in $A_{0.7}A'_{0.3}\text{MnO}_3$ manganites fitted by the function $T_C = A \exp(-B\delta_{JT})$. The error bars are within the symbol sizes.

comes from equation (2) and the observed linear relationship between E_{JT} and δ_{JT} that the T_C (δ_{JT}) dependence should follow the exponential behaviour $T_C = A \exp(-B\delta_{JT})$, in agreement with the observation (figure 3). The parameters A and B are related to those of equation (2) as $A \propto W$ and $B \propto \gamma/\hbar\omega$. The values $A = 308.82$ K and $B = 68.66 \text{ \AA}^{-1}$ were obtained from the fit to experimental data.

Previously it was found that the change of T_C value in manganites correlates with the variation of $\langle r_A \rangle$ [6] and also r_A variance $\sigma^2 = \sum_i y_i (r_A^i)^2 - \langle r_A \rangle^2$, where the y_i are the fractional occupancies of different A-site elements [19]. The static JT distortion parameter increases nearly linearly with decrease of $\langle r_A \rangle$ (figure 4) but shows no obvious dependence on the σ^2 value (figure 4) for the studied compounds.

Among the $A_{0.7}A'_{0.3}\text{MnO}_3$ manganites the largest Curie temperatures are observed in compounds with the rhombohedral crystal structure of $R\bar{3}c$ symmetry. For instance, the Curie temperature $T_C = 370$ K for rhombohedral $\text{La}_{0.7}\text{Sr}_{0.3}\text{MnO}_3$ is much larger in comparison with those for the considered orthorhombic lanthanum-based compounds $\text{La}_{0.7}\text{Ca}_{0.17}\text{Sr}_{0.13}\text{MnO}_3$ ($T_C = 309$ K [6]), $\text{La}_{0.7}\text{Ca}_{0.3}\text{MnO}_3$ ($T_C = 270$ K [13]) and $\text{La}_{0.525}\text{Pr}_{0.175}\text{Ca}_{0.3}\text{MnO}_3$ ($T_C = 200$ K [16]). One of main reasons for this effect may be the absence of the static long range cooperative JT distortion which is forbidden by the $R\bar{3}c$ symmetry, which implies that MnO_6 octahedra are isotropic with equal Mn–O bond lengths and Mn–O–Mn angles. Consequently, the electron–phonon coupling effects are suppressed in rhombohedral manganites in comparison with the orthorhombic ones, where such effects lead to the reduction of Curie temperature values. The study of manganites $\text{La}_{2/3}(\text{Ca}_{1-y}\text{Sr}_y)_{1/3}\text{MnO}_3$ [11] also revealed that enhanced lattice effects are responsible for different properties of the samples with the orthorhombic structure in comparison with those having the rhombohedral structure.

3. Conclusions

The results of our study show that the Curie temperature of manganites $A_{0.7}A'_{0.3}\text{MnO}_3$ ($A = \text{La}, \text{Pr}, \text{Nd}; A' = \text{Ca}, \text{Sr}$) is controlled by static long range cooperative JT distortion. The electron–phonon coupling effects become more pronounced with increase of the JT distortion parameter due to relevant increase of the JT polaron binding energy. The JT distortion parameter shows

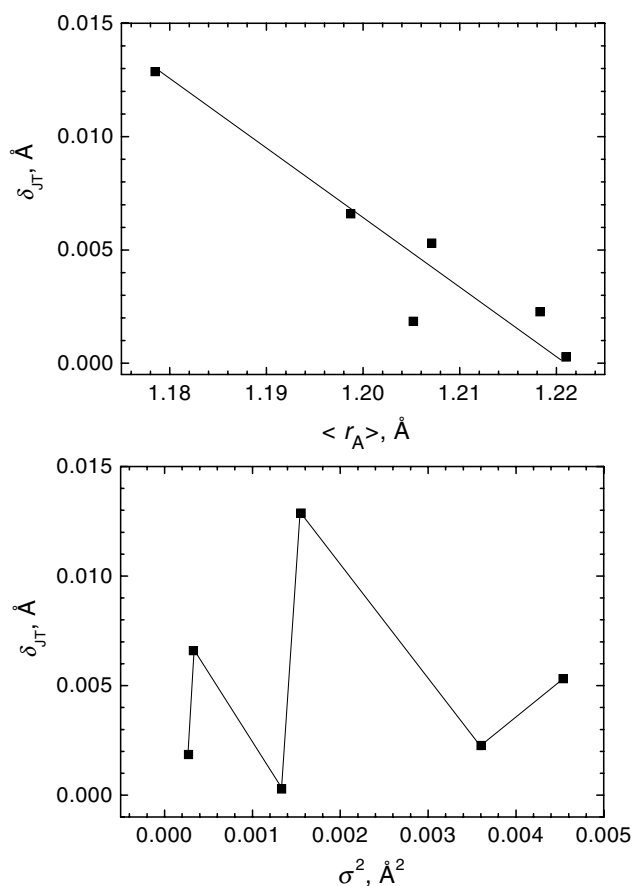


Figure 4. The static JT distortion parameter as a function of the average A-site ionic radius $\langle r_A \rangle$ (top) and its variance σ^2 (bottom) for $A_{0.7}A'_{0.3}\text{MnO}_3$ manganites. The error bars are within the symbol sizes.

close correlation with the average A-site ionic radius and increases with decrease of $\langle r_A \rangle$. No certain correlation between δ_{JT} and the r_A variance σ^2 was observed.

Acknowledgment

The work was supported by the Russian Foundation for Basic Research, grant 03-02-16879.

References

- [1] Dagotto E, Hotta T and Moreo A 2001 *Phys. Rep.* **344** 1
- [2] Zener C 1951 *Phys. Rev.* **82** 403
- [3] Anderson P W and Hasegawa H 1955 *Phys. Rev.* **100** 675
- [4] De Gennes P-G 1960 *Phys. Rev.* **118** 141
- [5] Furukawa N 1999 *Physics of Manganites* ed T A Kaplan and S D Mahanti (New York: Kluwer–Academic/Plenum) pp 1–38
Furukawa N 1998 *Preprint* cond-mat/9812066
- [6] Hwang H Y, Cheong S-W, Radaelli P G, Marezio M and Batlogg B 1995 *Phys. Rev. Lett.* **75** 914

-
- [7] Fontcuberta J, Laukhin V and Obradors X 1999 *Phys. Rev. B* **60** 6266
- [8] Hwang H Y, Palstra T T M, Cheong S-W and Batlogg B 1995 *Phys. Rev. B* **52** 15046
- [9] Laukhin V, Fontcuberta J, García-Muñoz J L and Obradors X 1997 *Phys. Rev. B* **56** R10009
- [10] Harrison W A 1980 *The Electronic Structure and Properties of Solids* (San Francisco, CA: Freeman)
- [11] Mira J, Rivas J, Hueso L E, Rivadulla F, López Quintela M A, Señarís Rodríguez M A and Ramos C A 2001 *Phys. Rev. B* **65** 024418
- [12] Radaelli P G, Iannone G, Marezio M, Hwang H Y, Cheong S-W, Jorgensen J D and Argyriou D N 1997 *Phys. Rev. B* **56** 8265
- [13] Hibble S J, Cooper S P, Hannon A C, Fawcett I D and Greenblatt M 1999 *J. Phys.: Condens. Matter* **11** 9221
- [14] Boujelben W, Ellouze M, Cheikh-Rouhou A, Pierre J, Cai Q, Yelon W B, Shimizu K and Dubourdieu C 2002 *Phys. Status Solidi a* **191** 243
- [15] Millange F, Caignaert V, Mather G, Suard E and Raveau B 1996 *J. Solid State Chem.* **127** 131
Pattabiraman M, Murugaraj P, Rangarajan G, Dimitropoulos C, Ansermet J-Ph, Papavassiliou G, Balakrishnan G, Paul D McK and Lees M R 2002 *Phys. Rev. B* **66** 224415
- [16] Radaelli P G, Marezio M, Hwang H Y, Cheong S-W and Batlogg B 1996 *Phys. Rev. B* **54** 8992
- [17] Lorenz B, Heilman A K, Wang Y S, Xue Y Y, Chu C W, Zhang G and Franck J P 2001 *Phys. Rev. B* **63** 144405
- [18] Garbarino G, Acha C, Vega D, Leyva G, Polla G, Martin C, Maignan A and Raveau B 2004 *Phys. Rev. B* **70** 014414
- [19] Rodriguez-Martinez L M and Attfield J P 1996 *Phys. Rev. B* **54** R15622